PET of CXCR4 Expression by a ^{68}Ga-Labeled Highly Specific Targeted Contrast Agent

Eleni Gourni[1], Oliver Demmer[2], Margret Schottelius[1], Calogero D'Alessandria[3], Stefan Schulz[4], Ingrid Dijkgraaf[3], Udo Schumacher[5], Markus Schwaiger[3], Horst Kessler[2,6], and Hans-Jürgen Wester[1]

[1]Pharmaceutical Radiochemistry, Technische Universität München, Garching, Germany; [2]Institute for Advanced Study, Technische Universität München, Garching, Germany; [3]Nuklearmedizinische Klinik und Poliklinik, Klinikum rechts der Isar, Technische Universität München, München, Germany; [4]Institut für Pharmakologie und Toxikologie, Universitätsklinikum Jena, Jena, Germany; [5]Institute for Anatomy II, Universitätsklinikum Hamburg-Eppendorf, Hamburg, Germany; and [6]Chemistry Department, Faculty of Science, King Abdulaziz University, Jeddah, Saudi Arabia

The overexpression of the chemokine receptor CXCR4 plays an important role in oncology, since together with its endogenous ligand, the stromal cell–derived factor (SDF1-α), CXCR4 is involved in tumor development, growth, and organ-specific metastasis. As part of our ongoing efforts to develop highly specific CXCR4-targeted imaging probes and with the aim to assess the suitability of this ligand for first proof-of-concept studies in humans, we further evaluated the new ^{68}Ga-labeled high-affinity cyclic CXCR4 ligand, ^{68}Ga-CPCR4-2 (*cyclo*(D-Tyr^1-[*N*Me]-D-Orn^2-[4-(aminomethyl) benzoic acid,^{68}Ga-DOTA]-Arg^3-2-Nal^4-Gly^5)). **Methods:** Additional biodistribution and competitions studies in vivo, dynamic PET studies, and investigations on the metabolic stability and plasma protein binding were performed in nude mice bearing metastasizing OH1 human small cell lung cancer xenografts. CXCR4 expression on OH1 tumor sections was determined by immunohistochemical staining. **Results:** ^{nat}Ga-CPCR4-2 exhibits high CXCR4 affinity with a half maximum inhibitory concentration of 4.99 ± 0.72 nM. ^{68}Ga-CPCR4-2 showed high in vivo stability and high and specific tumor accumulation, which was reduced by approximately 80% in competition studies with AMD3100. High CXCR4 expression in tumors was confirmed by immunohistochemical staining. ^{68}Ga-CPCR4-2 showed low uptake in nontumor tissue and particularly low kidney accumulation despite predominant renal excretion, leading to high-contrast delineation of tumors in small-animal PET studies. **Conclusion:** The small and optimized cyclic peptide CPCR4-2 labeled with ^{68}Ga is a suitable tracer for targeting and imaging of human CXCR4 receptor expression in vivo. The high affinity for CXCR4, its in vivo stability, and the excellent pharmacokinetics recommend the further evaluation of ^{68}Ga-CPCR4-2 in a proof-of-concept study in humans.

Key Words: PET; ^{68}Ga; CXCR4; cancer metastasis

J Nucl Med 2011; 52:1803–1810
DOI: 10.2967/jnumed.111.098798

Metastasis, a key step in cancer development, is the leading cause of death for most patients with cancer. Consequently, sensitive and early detection of the metastatic potential of a primary tumor and of metastatic spread could have major impact on the chosen therapeutic strategy and thus on the prognosis of the disease. One promising target that is a key player in the process of cancer metastasis is the chemokine receptor CXCR4. CXCR4 belongs to the family of G-protein–coupled receptors and directs cell locomotion toward higher concentrations of chemokines (*1,2*). Physiologically, CXCR4 is essential for the hematopoiesis, organogenesis, and vascularization during development (*3*). However, CXCR4 is also involved in various diseases such as the entry of HIV-1 (*4*) and several inflammatory conditions (*5*).

The important role of CXCR4 and of its endogenous ligand, stromal cell–derived factor (SDF1-α) (also named CXCL12), in oncology relies on 2 major factors: first, on SDF1-α binding to CXCR4, the G protein complex is activated and triggers parallel signal transduction cascades, leading to cancer cell proliferation, migration, and survival (*1,2*). Furthermore, CXCR4 expression on primary tumor cells directs circulating cancer cells to those organs that express SDF1-α, such as lung, liver, and bone marrow, resulting in organ-specific metastasis (*2,6–8*).

Many efforts have been directed toward the development of suitable CXCR4 imaging probes, most of which are derived from SDF1-α (*9–11*). The first downsized CXCR4 ligand, T140 (Arg^1-Arg^2-Nal^3-*cyclo*(Cys^4-Tyr^5-Arg^6-Lys^7-D-Lys^8-Pro^9-Tyr^{10}-Arg^{11}-Cit^{12}-Cys^{13})-Arg^{14}), was shown to exhibit strong antagonistic action, which is primarily mediated by the 4 N- and C-terminal residues Nal^3, Tyr^5, Arg^{14}, and Arg^2 (*10*). On the basis of this structure–activity relationship, cyclic pentapeptides such as FC131 (*cyclo*(D-Tyr^1-Arg^2-Arg^3-2-Nal^4-Gly^5)), displaying improved metabolic stability as well as potent CXCR4 antagonism, have been developed (*12*). ^{124}I-FC131 was the first CXCR4-directed PET agent in preclinical evaluation (*13*). It showed high accumulation in the CXCR4-positive tumor in an animal model and high focal uptake in lung micrometastases.

Received Sep. 29, 2011; revision accepted Sep. 29, 2011.
For correspondence and reprints contact: Hans-Jürgen Wester, Pharmaceutical Radiochemistry, Technische Universität München, Meissner-Strasse 3, D-85748 Garching, Germany.
E-mail: h.j.wester@tum.de

Its applicability for whole-body CXCR4 imaging, however, is severely hampered by the high lipophilicity and consequently high hepatic and intestinal uptake (*13–15*).

Other recently developed CXCR4-targeted nuclear imaging probes, including the T140 analogs ^{111}In-diethylenetriaminepentaacetic acid (DTPA)-Ac-TZ14011 (*16*) and ^{18}F-T140 (*17*), show high accumulation and retention in liver and spleen and low tumor-to-background ratios. The cyclam derivative ^{64}Cu-AMD3100 shows significantly higher tumor accumulation and improved tumor-to-background ratios. Its applicability for patient imaging, however, is challenged by high hepatic accumulation, leading to tumor-to-liver ratios less than 1 (*18,19*). SPECT/CT was applied for the detection of CXCR4 receptors using ^{125}I-labeled antibodies (*20*). ^{99m}Tc-labeled SDF-1α was used as a sensitive and specific probe for CXCR4 expression under different physiologic and pathologic states (*21*).

On the basis of our results with ^{124}I-FC131 and triggered by the advantageous features of ^{68}Ga as a PET radionuclide, we recently developed a ^{68}Ga-labeled cyclic CXCR4-binding pentapeptide, ^{68}Ga-CPCR4-2 (*cyclo*(D-Tyr^1-D-[*N*Me]Orn^2-[AMBS-DOTA]-Arg^3-2-Nal^4-Gly^5)), (AMBS: 4-(aminomethyl) benzoic acid) (*22*). However, because conjugation of the relatively bulky radiometal chelate to the small cyclic pentapeptide was found to substantially affect the binding affinity, identification of the optimal site of attachment and optimization of suitable linker units were necessary. On the basis of our *cyclo*(D-Tyr^1-Orn^2-Arg^3-2-Nal^4-Gly^5)-scaffold, more than 150 mono- and multimeric pentapeptides were screened to explore the flexibility of the CXCR4 binding pocket (*14,15,22,23*).

In the most promising candidate, CPCR4-2, the [*N*Me]-D-Orn^2 side chain was functionalized with DOTA via an AMBS (HOOC-C_6H_4-CH_2-NH_2) linker (Fig. 1). As determined in CXCR4-expressing Jurkat cells, ^{nat}Ga-CPCR4-2 showed high affinity to CXCR4. In a competition binding assay, specific binding of ^{125}I-FC131 to Jurakt cells was inhibited by ^{nat}Ga-CPCR4-2 with a half maximal inhibitory concentration (IC_{50}) of 5 ± 1 nM. Furthermore, initial biodistribution studies in mice bearing human small cell lung cancer tumors revealed CXCR4-specific tumor uptake, fast renal excretion, and high tumor-to-muscle ratios at 1 and 2 h after injection (*22*). In addition to those initial experiments, we herein describe the further evaluation of ^{68}Ga-CPCR4-2, with a particular focus on additional pharmacologic studies that allow us to assess the suitability of this tracer for a proof-of-concept study in humans — that is, the metabolic stability, lipophilicity, plasma protein binding, immunohistochemical analysis, extended biodistribution study, extended blockade study, and dynamic PET studies in mice bearing CXCR4-overexpressing human small cell lung cancer OH1 tumors.

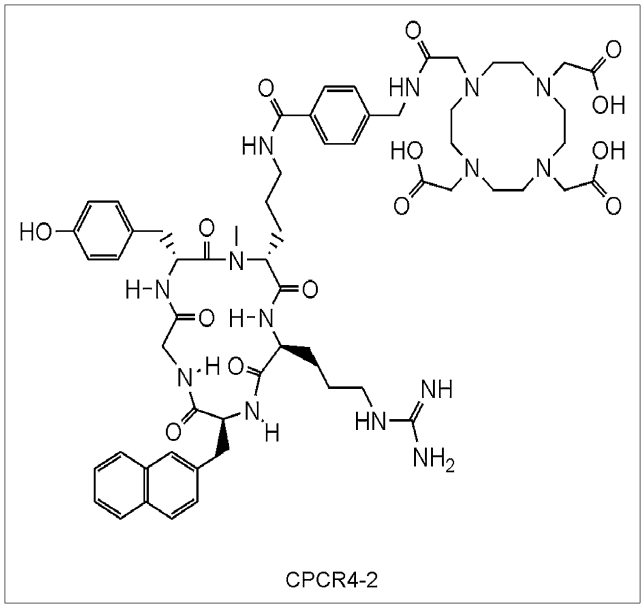

FIGURE 1. Chemical structure of CPCR4-2.

MATERIALS AND METHODS

Radiolabeling of CPCR4-2 with ^{68}Ga

^{68}Ga-CPCR4-2 was prepared on a fully automated system (Scintomics GmbH) as previously described (*22*). Briefly, the eluate (1.1–1.3 GBq, 1.25 mL) of a ^{68}Ge/^{68}Ga generator (iThemba LABS) was added to a solution of 15 nmol CPCR4-2 and 600 mg of *N*-(2-hydroxyethyl)piperazine-*N*′-(2-ethanesulfonic acid) (Merck) in 0.5 mL of H_2O and reacted for 5 min at 95°C (pH 3.2–3.3). ^{68}Ga-CPCR4-2 was immobilized on a SepPak C18 cartridge (Waters), washed with H_2O, and eluted with 1 mL of EtOH.

Separation of ^{68}Ga-CPCR4-2 from Unlabeled CPCR4-2 Precursor

As a compound with high affinity to a G-protein–coupled receptor also responsible for the binding of stem cells in bone marrow stem cell niches, we decided to prepare the tracer in a maximum specific activity. Thus, ^{68}Ga-CPCR4-2 was separated from unlabeled precursor using reversed-phase high-performance liquid chromatography (RP-HPLC) on a semipreparative RP18 Multosphere column (250 × 10 mm), applying a linear gradient of 49%–60% solvent B in 20 min at a flow rate of 5 mL/min (solvent A, 0.2 M ammonium formate; solvent B, MeOH). Ultraviolet detection was performed using a Linear UVIS 200 detector at 220 nm. For radioactivity measurement, a Na(TI) well-type scintillation counter (Ace Mate 925-Scint; EG&G Ortec) was used. After RP-HPLC purification, the product fraction containing no-carrier-added (NCA) ^{68}Ga-CPCR4-2 was evaporated in vacuo, redissolved with 5 mL of H_2O, immobilized on a SepPak C18 cartridge, washed twice with H_2O (3 mL), and eluted with 2 mL of EtOH. After solvent evaporation in vacuo, ^{68}Ga-CPCR4-2 was reconstituted in phosphate-buffered saline (PBS; pH 7.4) for further use.

Quality Control of Radiolabeled Product

Chemical and radiochemical purity of ^{68}Ga-CPCR4-2 were determined using an analytic Nucleosil 100–5 C18 column (125 × 4.6 mm) at a flow rate of 1 mL/min (gradient, 49%–60% solvent B in 20 min; solvent A, 0.2 M ammonium formate; solvent B, MeOH).

The presence of free $^{68}Ga^{3+}$ and $^{68}Ga^{3+}$-colloid in the ^{68}Ga-CPCR4-2 preparation was quantified by radio-thin-layer chroma-

tography (radio-TLC) using silica gel 60 plates and 2 different mobile phase systems (*22*).

Lipophilicity

The lipophilicity of ^{68}Ga-CPCR4-2 was determined as reported previously (*24*).

Cell Cultures

The human T lymphocyte Jurkat cell line was purchased from American Type Culture Collection. The human small cell lung cancer line OH1, which forms multiple metastases in the lung approximately 2–3 wk after tumor cell inoculation and subsequent growth, was provided by Dr. Udo Schumacher. Both cell lines were grown in RPMI 1640 medium supplemented with 10% fetal calf serum. Cell lines were cultured at 37°C in a humidified 5% CO_2 atmosphere. All medium and supplements were obtained from Biochrom.

For cell counting, a CASY1-TT cell counter and an analyzer system (Schärfe System GmbM) were used.

Competition Binding Studies

Competition binding experiments were performed using Jurkat cells with ^{125}I-FC131 as a radioligand as previously described (*22*).

Animal Models

Female athymic nude mice (age, 6–8 wk; weight, 25–30 g) were purchased from Charles River. The animals were inoculated with 5×10^6 OH1 cells subcutaneously in 100 μL of medium into the right shoulder. After an average of 3 wk, tumor weight reached 0.8–1.5 g, and the animals were used for biodistribution and PET studies. All animal experiments were approved by local authorities and were in compliance with the institutions guidelines.

Metabolite Analysis and Plasma Protein Binding Study

OH1 mice were injected with approximately 12–14 MBq of ^{68}Ga-CPCR4-2 in a total volume of 0.1 mL of PBS and sacrificed 30 min after injection. Blood was collected in heparinized tubes and centrifuged (5 min, 1,677*g*; Heraeus Sepatech Biofuge 15) for plasma isolation. Liver, kidney, and tumor were dissected, rinsed with 0.9% NaCl, and immersed in ice-cold 50 mM Tris/0.2 M sucrose buffer, pH 7.4. The organs were subsequently homogenized with a manual homogenizer for 5 min, followed by centrifugation (10 min, 9,660*g*), and the supernatants were used for further evaluation. Samples (300 μL) of plasma and homogenized organs were transferred to an ultrafiltration device (Vivacon 500; 30,000 molecular weight cutoff [Sartorius Stedium Biotech GmbH]), followed by centrifugation (10 min, 9,660*g*) for the separation of proteins. Samples from the ultrafiltrate and ^{68}Ga-CPCR4-2 solution were applied to a preparative TLC glass plate (PTLC silica gel with F_{254} indicator on glass plates with a 4 × 20 cm preconcentration zone) for the quantification of the radiolabeled metabolic species. A 6:4 (v/v) mixture of MeOH/0.2 M ammonium formate was used as the mobile phase. Radio-TLC detection was performed using a Phospho-Imager (CR 35 BIO; Isotopenmeßgeräte GmbH). Images were analyzed using AIDA Image Analyzer software (Raytest).

Plasma protein binding at 30 min after injection of ^{68}Ga-CPCR4-2 was determined by ultrafiltration as described previously (*25*).

Biodistribution Studies

In addition to the blockade experiment with FC131 previously described (*22*) and to evaluate the efficacy of a structurally completely different competitor in vivo, we performed a blockade study with the partial CXCR4 agonist AMD3100 (*26*) (50 μg/mouse). Furthermore, the biodistribution study of ^{68}Ga-CPCR4-2 (*22*) was extended by an additional time point at 10 min after injection.

Preparation of Frozen Tumor Sections

Immediately after dissection, tumors were frozen on dry ice and embedded in optimal-cutting-temperature (OCT) medium (4583; Sakura Finetek). Contiguous frozen sections (7 μm) were cut from the central part of the tumor using an HM500 cryostat microtome (Microm International GmbH) and adhered to poly-L-lysine–coated glass microscope slides. Frozen sections were stored at −80°C until use.

Immunolocalization of CXCR4 Receptor in OH1 Primary Tumor

The expression of CXCR4 in primary OH1 tumor was confirmed by performing immunohistochemical staining for CXCR4 and using the rabbit monoclonal anti-CXCR4 antibody clone UMB-2 (kindly provided by Dr. Stefan Schulz, Institute for Pharmakology and Toxicology, University Hospital Jena, Germany). Briefly, slides were air-dried, fixed in 10% formalin for 30 min, incubated in 0.3% H_2O_2 to block endogenous peroxidase, and incubated overnight at 4°C with rabbit monoclonal anti-CXCR4 antibody UMB-2 (dilution, 1:10). Detection of the primary antibody was performed using biotinylated antirabbit IgG, followed by incubation with peroxidase-conjugated avidin (Vector ABC Elite kit; Vector Laboratories). As a chromogen, 3-amino-9-ethylcarbazole in acetate buffer (BioGenex) was used. Sections were rinsed, counterstained with Mayer hematoxylin (Sigma-Aldrich Inc.), and mounted in Vectamount mounting medium (Vector Laboratories). For immunohistochemical controls, the primary antibody was adsorbed for 2 h at room temperature with the immunizing peptide (10 μg/mL) (*27*). Images were acquired at ×200 and ×600 magnification using a Zeiss Axio Imager.A1 microscope and captured with a Progres C5-Kamera and Progres Mac Capture Pro 2.7 software (Jenoptic).

PET Camera Imaging

Mice bearing OH1 xenografts were anesthetized using isoflurane anesthesia and injected with (7.4–14.8 MBq) of ^{68}Ga-CPCR4-2 in 100 μL of PBS into the tail vein. PET scans were obtained using an Inveon PET scanner (Siemens). Dynamic imaging was performed immediately after injection with the following acquisition frames: 5 × 60, 5 × 300, 6 × 600, and 1 × 1,200 s, amounting to a total imaging time of 110 min. Competition experiments were performed by coinjection of the tracer with 50 μg of FC131 or AMD3100 in a total volume of 150 μL of PBS. Static images were obtained from 90 to 110 min after injection. All images were corrected for ^{68}Ga decay and reconstructed by a 3-dimensional ordered-subsets expectation maximum algorithm. No attenuation correction was applied. Images were analyzed using Inveon software.

RESULTS

Radiolabeling of CPCR4-2 with ^{68}Ga

We recently described the development and radiolabeling of the CXCR4 directed cyclic DOTA-conjugated pentapeptide CPCR4-2 (*22*). Standard reaction conditions (15 nmol of peptide, starting activities of 1.1–1.3 GBq) yielded ^{68}Ga-CPCR4-2 in 50% radiochemical yield and greater than 95% radiochemical purity within 17 min. To avoid pharmaco-

logic effects, such as stem cell mobilization, in future proof-of-concept studies in humans and to use the same experimental conditions in the preclinical evaluation, we isolated ^{68}Ga-CPCR4-2 from the excess unlabeled CPCR4-2 by RP-HPLC. Despite the additional HPLC purification step (45 min), decay-corrected yields for NCA ^{68}Ga-CPCR4-2 were high (24.5% ± 3.5% based on ^{68}Ga starting activity and 73% ± 3% based on crude ^{68}Ga-CPCR4-2 [n = 5]).

Lipophilicity

With a $\log P_{octanol/PBS}$ of −2.90 ± 0.08, ^{68}Ga-CPCR4-2 shows greatly enhanced hydrophilicity, as compared with ^{125}I-FC131, which showed a $\log P_{octanol/PBS}$ of −0.35 ± 0.02 (*14,15*). (Lipophilicity = the logarithm of the partition coefficient P, where P is the ratio of the distribution of a compound in 2 solvents, here octanol and PBS.)

Competition Binding Studies

IC_{50} data obtained for ^{nat}Ga-CPCR4-2, CPCR4-2, and FC131 in Jurkat cells are summarized in Table 1. Despite the fundamental structural modifications introduced into ^{nat}Ga-CPCR4-2 as compared with FC131, the affinities of both peptides were found to be nearly identical, whereas the comparably small structural differences between uncomplexed CPCR4-2 and ^{nat}Ga-CPCR4-2 resulted in a significant effect on CXCR4 binding affinity.

Plasma Protein Binding Study and Metabolite Analysis

To estimate the bioavailability of ^{68}Ga-CPCR4-2 in circulation, the extent of plasma protein binding was determined. Approximately two thirds (64% ± 4%) of the circulating ^{68}Ga activity were found to be bound to plasma proteins. As demonstrated by radio-TLC metabolite analysis of plasma samples 30 min after injection of ^{68}Ga-CPCR4-2, the remaining circulating activity exclusively consists of intact radiotracer. Also, in tissue homogenates from liver, kidney, and tumor, only intact ^{68}Ga-CPCR4-2 was detected at 30 min after injection, demonstrating the stability of ^{68}Ga-CPCR4-2 toward in vivo degradation.

Biodistribution Studies

The biodistribution of ^{68}Ga-CPCR4-2 in OH1 mice was extended by an early time point at 10 min after injection (Table 2). Radioactivity was efficiently and rapidly cleared from the blood via the kidneys, with low retention of radioactivity in kidney tissue. Except for the early time point at 10 min after injection, the accumulation of ^{68}Ga-CPCR4-2 was higher in tumor than in any other organ, with a maximum at 60 min after injection. Accumulation of radioactivity in the liver and spleen, organs with high expression of CXCR4 messenger RNA (*28*), was low, with absolute values of 1.85 ± 0.24 %ID/g and 0.69 ± 0.09 %ID/g at 60 min after injection, respectively. Blockade studies in vivo with excess FC131 (*22*) and more effectively in this study with AMD3100 demonstrate the specificity of ^{68}Ga-CPCR4-2 uptake by human CXCR4 receptors expressed on the human small cell lung cancer model. The administration of the competing dose of AMD3100 resulted in a reduction of the ^{68}Ga-CPCR4-2 uptake in tumor by approximately 80%.

TABLE 1
IC_{50} of Selected CXCR4 Ligands for Binding of ^{125}I-FC131 to CXCR4-Expressing Jurkat Cells

Compound	IC_{50} (nM)
FC131	4.43 ± 0.82
CPCR4-2	177
^{nat}Ga-CPCR4-2	4.99 ± 0.72

Data are mean ± SD of 3 experiments, except for values greater than 80 nM.

Immunolocalization of CXCR4 on OH1 Frozen Sections

Frozen sections from OH1 tumor, dissected from a mouse that had previously undergone PET using ^{68}Ga-CPCR4-2, were cut and stained for immunolocalization of CXCR4. Positive staining was found on the whole section, with variable intensity. The staining was clearly associated with the plasma membrane of OH1 tumor cells. The CXCR4 specificity of the staining was proven by incubating sections with the anti-CXCR4 antibody previously adsorbed with its immunizing peptide (Fig. 2).

PET

Representative PET images obtained in OH1 mice on injection of ^{68}Ga-CPCR4-2 are shown in Figure 3. The experimental tumors were clearly delineated within the first 30 min after injection of the radiopeptide. Tumor uptake was very high and persistent within the 120-min time frame; the initial background uptake of ^{68}Ga-CPCR4-2 in the excretion organs (liver, kidneys) rapidly decreased over time (Figs. 3 and 4). Predominant urinary excretion of the tracer is represented by the high focal activity concentration in the urinary bladder at all time points. To visualize the extent of CXCR4-specific tumor uptake of ^{68}Ga-CPCR4-2, PET competition studies using FC131 and AMD3100 as competitors were also performed. These images well represent the differences in overall biodistribution, which had already been encountered in the biodistribution studies—that is, a reduction of tumor uptake by a blocking dose of both FC131 and AMD3100, which is accompanied by delayed overall activity excretion in the case of FC131.

DISCUSSION

Because of its availability from generator systems and the relative ease of radiometallation chemistry, the positron emitter ^{68}Ga has gained increasing interest in the field of radiopharmaceutical chemistry. These factors and our previous experience with radiolabeled CXCR4-binding peptides as powerful imaging probes for the detection of primary and metastatic tumors prompted us to develop ^{68}Ga-CPCR4-2.

TABLE 2
Biodistribution of ^{68}Ga-CPCR4-2 in OH1 Mice at 10, 60, and 120 Minutes After Injection

Organ	Time after injection (min)			
	10 (n = 5)	60 (n = 8) (*22*)	120 (n = 3) (*22*)	60 (after injection of 50 μg AMD3100; n = 5)
Blood	6.35 ± 0.61	1.08 ± 0.27	0.58 ± 0.14	0.96 ± 0.14
Heart	3.37 ± 0.39	0.60 ± 0.16	0.29 ± 0.10	0.50 ± 0.07
Lung	6.75 ± 0.93	1.41 ± 0.26	2.85 ± 2.69	1.41 ± 0.14
Liver	4.49 ± 0.60	1.85 ± 0.24	1.48 ± 0.31	1.06 ± 0.17
Pancreas	1.45 ± 0.06	0.30 ± 0.07	0.21 ± 0.02	0.25 ± 0.05
Spleen	2.54 ± 0.47	0.69 ± 0.09	0.65 ± 0.25	0.43 ± 0.10
Kidney	14.66 ± 2.07	3.06 ± 0.63	2.07 ± 0.46	2.88 ± 0.45
Adrenal glands	2.54 ± 1.12	0.83 ± 0.55	0.50 ± 0.15	0.70 ± 0.22
Stomach	3.45 ± 0.13	0.72 ± 0.26	0.46 ± 0.12	0.82 ± 0.45
Intestine	1.69 ± 0.15	0.45 ± 0.11	0.36 ± 0.04	0.47 ± 0.13
Muscle	1.25 ± 0.23	0.38 ± 0.09	0.28 ± 0.17	0.30 ± 0.13
Tumor	4.55 ± 1.10	6.16 ± 1.16	4.63 ± 1.54	1.35 ± 0.27
Tumor-to-organ ratio				
Tumor to blood	0.73 ± 0.21	5.81 ± 0.88	8.03 ± 2.59	1.41 ± 0.25
Tumor to liver	1.04 ± 0.32	3.31 ± 0.32	3.06 ± 0.48	1.27 ± 0.09
Tumor to kidney	0.32 ± 0.10	2.03 ± 0.19	2.36 ± 1.14	0.47 ± 0.04
Tumor to muscle	3.68 ± 0.90	16.55 ± 3.84	18.49 ± 7.29	3.62 ± 0.83

We recently reported on the development of a series of new radioiodinated, radiofluorinated, and radiometallated cyclic pentapeptides (*22*). The *N*-methylated analog *cyclo*(D-Tyr^1-[*N*Me]-D-Orn^2-Arg^3-2-Nal^4-Gly^5) was derived from a pentapeptide library (*14,15*) and was found to exhibit high affinity for CXCR4 (IC_{50} = 6.15 ± 0.84 nM). In a next step, direct conjugation of this peptide with a chelator suitable for a variety of radiometals to the [*N*Me]-D-Orn^2 side chain was performed. Though not optimal (*29*) for $^{68}Ga^{3+}$-ion, DOTA was chosen because it provides maximum flexibility with respect to future diverse applicability with other radiometals such as ^{90}Y, ^{177}Lu, or ^{111}In. Unfortunately, the direct attachment of the bulky gallium-DOTA metal chelate to *cyclo*(D-Tyr^1-[*N*Me]-D-Orn^2-Arg^3-2-Nal^4-Gly^5) resulted in a loss of CXCR4 affinity by a factor of 135. Thus, a variety of spacers were introduced and tested, among which AMBS was found to be most suitable. Although the affinity of uncomplexed CPCR4-2 to CXCR4 was found to be relatively low, ^{nat}Ga-CPCR4-2 showed an increase in CXCR4 affinity by a factor of 35, which may be explained by the fundamental structural differences and by the overall charge and charge distribution induced by the complexation of gallium (*30*).

In this work, we further evaluate our previously published cyclic ^{68}Ga-labeled CXCR4-binding pentapetide ligand, ^{68}Ga-CPCR4-2, with the aim to assess this tracer for first proof-of-concept studies in humans. ^{68}Ga-CPCR4-2 is available in high radiochemical purity and good radiochemical yields. Specific activities in the range of those achieved for patient doses of ^{68}Ga-DOTATOC (*31,32*), for which 7–35 nmol of precursor peptide are currently used, are easily achievable using standard reaction conditions (15 nmol of peptide). Given the fact, however, that the tumor uptake in animal models is highly dependent on the specific activity of the radiopeptide injected (*32*) and with the aim to use conditions similar to those projected for the first in vivo studies in humans (i.e., minimizing the effects of stem cell mobilization), we chose to prepare ^{68}Ga-CPCR4-2 for the preclinical assessment on an NCA level via HPLC purification. Especially when taking into account the relatively short half-life of ^{68}Ga, this step certainly represents an unwanted complication of the otherwise straightforward preparation of ^{68}Ga-CPCR4-2. We are confident, however, that this additional purification step may be obviated in the

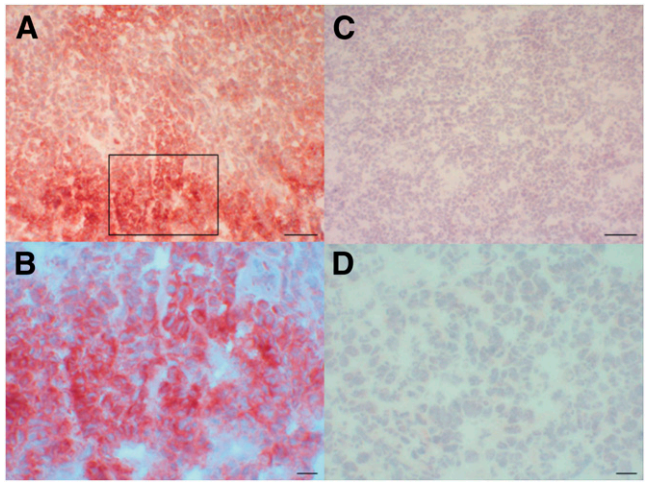

FIGURE 2. Immunohistochemical localization of CXCR4-expressing cells in frozen tissue sections from primary OH1 tumor. (A) Arbitrary region (x200). (B) Magnification of inset in A shows strong staining for CXCR4 around plasma membrane of OH1 tumor cells (x600). (C and D) When sections were incubated with antibody preadsorbed with its immunizing peptide, staining was completely abolished (x200 [C] and x600 [D]). Scale bars: 100 μm for A and C, 50 μm for B and D.

RGB

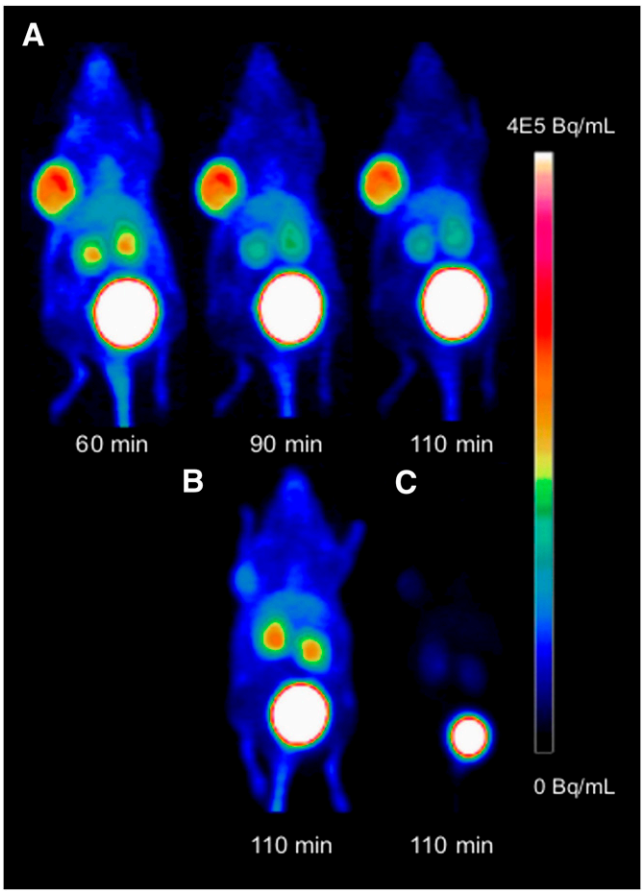

FIGURE 3. (A) PET dynamic imaging of OH1 mouse 0–110 min after injection of 9.6 MBq of ^{68}Ga-CPCR4-2. (B and C) PET summation images 90–110 min after coinjection of 50 μg of FC131 and 13.7 MBq of ^{68}Ga-CPCR4-2 (B) or coinjection of 50 μg of AMD3100 and 7.4 MBq of ^{68}Ga-CPCR4-2 (C).

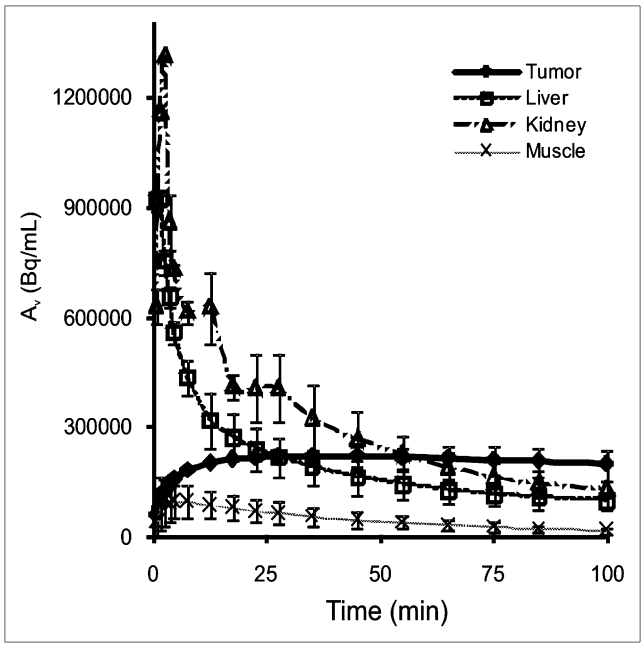

FIGURE 4. Time–activity curves acquired via dynamic small-animal PET 0–100 min after injection of ^{68}Ga-CPCR4-2 in OH1 tumor–bearing nude mice (n = 3).

future using optimized chelator systems that require considerably lower peptide concentrations.

The in vivo pharmacokinetics of ^{68}Ga-CPCR4-2 is characterized by fast tracer clearance from nontarget tissues and rapid accumulation in the OH1 xenografts, with maximum uptake at 60 min after injection. In comparative in vitro studies at 4°C and 37°C, ^{125}I-FC131 was found to be exclusively bound to the cell surface of tumor cells and not actively internalized, indicating an antagonistic profile. Data from ex vivo immunohistochemistry of CXCR4 expression demonstrated exclusive CXCR4 localization at the cell membrane (Fig. 2), supporting the assumption that ^{nat}Ga-CPCR4-2 also presents an antagonistic profile.

In vivo competition by coinjection of a blocking dose of AMD3100 led to the expected reduction in tumor uptake, without affecting activity accumulation in other organs. In contrast, a previous study obtained with FC131 (*22*) revealed sustained plasma activity and thus increased activity concentration in other tissues (Fig. 3). Whether this effect can fully or in part be attributed either to the aforementioned plasma protein binding of approximately 65% or to a general pharmacologic effect (*24*) needs to be further investigated. Nevertheless, a comparison of tumor or nontumor ratios obtained under AMD3100- and FC131-blocking conditions (Table 2) reveals superior CXCR4 blocking efficiency for FC131.

Similar to the native ligand SDF-1α, T140, CPCR4-analogous compounds, and AMD3100 are not CXCR4-selective ligands but also seem to bind the chemokine receptor subtype CXCR7 (*26,33*). Both CXCR4 and CXCR7 are frequently coexpressed on cancer cells (*34*). Coexpression of CXCR4 and CXCR7 has also been confirmed for the OH1 cell line used in this study. Western blot analysis revealed a CXCR4-to-CXCR7 expression ratio of 2.44. Thus, uptake of ^{68}Ga-CPCR4-2 in OH1 tumors via CXCR7 binding certainly contributes to overall tumor accumulation. Because FC131 and AMD3100 bind to both CXCR4 and CXCR7 (*26*), results from the competition studies reflect the contribution of CXCR4- and CXCR7-mediated tumor uptake and thus indicate the extent of CXCR4/CXCR7-specific binding. The use of recently developed CXCR4- and CXCR7-selective ligands (*33,35*) may allow the separation of the CXCR4/CXCR7 interplay.

Another interesting result is the low level of CXCR4-specific ^{68}Ga-CPCR4-2 binding to organs known to express high levels of CXCR4 messenger RNA in the mouse—for example, spleen and liver (*28*). Although ^{68}Ga-CPCR4-2 uptake in liver and spleen is reduced by a blocking dose of AMD3100 to 57% and 62% of control, respectively, this effect is far less pronounced than in the case of radiolabeled T140 analogs such as ^{111}In-Ac-TZ14011 (liver, 7%; spleen, 32% of control) (*16*) or ^{18}F-T140 (spleen, ≈ 20% of control) (*17*), indicating a higher species specificity of CPCR4-derived tracers for the human CXCR4 receptor.

On the basis of previous experiments showing the formation of lung micrometastases 2–3 wk after tumor inoculation in approximately 20% of the mice (*13*), we would have expected that lung uptake of ^{68}Ga-CPCR4-2 is at least partially blockable in the competition experiments. This, however, was not observed. Indications for the potential presence of lung metastases in the investigated group of animals were the large interindividual range of activity accumulation in the lung in the 120-min group (1.15–5.97 %ID/g) and previous autoradiography studies on cryosections of lungs from OH1 tumor–bearing mice demonstrating extremely high and not completely blockable focal tracer uptake in lung micrometastases even after injection of high doses of competitors (data not shown).

As anticipated from the substantially decreased lipophilicity of ^{68}Ga-CPCR4-2, as compared with ^{125}I-FC131, ^{68}Ga-CPCR4-2 shows almost exclusive renal excretion and low accumulation in the hepatobiliary system. Compared with ^{125}I-FC131, the tumor-to-liver and tumor-to-intestine ratios observed for ^{68}Ga-CPCR4-2 at 60 min after injection are increased (3.3 and 13.7 vs. 0.3 and 0.6 for ^{68}Ga-CPCR4-2 and ^{125}I-FC131, respectively), allowing high-contrast PET even in the abdominal region (Fig. 3).

The tumor-to-blood and tumor-to-muscle ratios found for ^{68}Ga-CPCR4-2 at 1 h after injection (5.8 ± 0.9 and 16.6 ± 3.8, respectively) are substantially higher than those found for other peptidic CXCR4 imaging agents. For example, values for ^{111}In-DTPA-Ac-TZ14001 are lower by a factor of 4.5–5 (1 h after injection, pancreatic carcinoma AsPC-1) (*16*). Without coadministration of a blocking dose of unlabeled peptide to repress ligand binding to red blood cells, tumor-to-blood and tumor-to-muscle ratios for ^{18}F-T140 were as low as 0.2 and 3, respectively (ovarian carcinoma CHO) (*17*). Data for ^{68}Ga-CPCR4-2 also compare well with the nonpeptidic ^{64}Cu-AMD3100, which, when evaluated in 2 human breast cancer models with intermediate to high receptor density (MDA-MB-231 expressing 6,833 ± 1,570 receptors per cell and DU4475 expressing 16,640 ± 5,128 receptors per cell), showed tumor-to-blood ratios of 1.9–3 and tumor-to-muscle ratios of 14–26 at 90 min after injection (*19*). Unfortunately, ^{64}Cu-AMD3100 exhibits high hepatic accumulation (tumor-to-liver ratios are < 1 at all time points), preventing the sensitive detection of liver metastases (*36*).

Interestingly, despite predominant renal excretion, ^{68}Ga-CPCR4-2 shows very low accumulation and no detectable retention in kidney tissue. This is even more surprising, because comparable peptidic constructs with identical net charge such as the somatostatin analog ^{68}Ga-DOTATOC show renal activity levels of 8.2 %ID/g at 4 h after injection (*37*). The high degree of ligand retention has been explained by efficient reabsorption of the peptides at the renal brush border membrane and subsequent trapping of charged degradation products (*38*). One explanation for the very low kidney retention of ^{68}Ga-CPCR4-2 might be its high metabolic stability, leading to direct excretion in the urine.

CONCLUSION

^{68}Ga-CPCR4-2 is the first CXCR4-directed PET agent that combines high CXCR4 affinity and thus high and persistent tumor uptake with suitable overall pharmacokinetics. Because of its hydrophilic nature, ^{68}Ga-CPCR4-2 is rapidly and predominantly cleared via the kidneys. Despite renal excretion, no significant retention of ^{68}Ga-CPCR4-2 in kidney tissue was observed. This study demonstrates the feasibility of tailoring target-specific CXCR4 imaging probes with an optimized imaging profile from a nonoptimized lead structure. ^{68}Ga-CPCR4-2 allows high-contrast PET of CXCR4-positive tumors and metastases even in the hepatic and abdominal region. We are confident that, on certain minor optimizations with respect to the labeling chemistry—that is, the overall yields—^{68}Ga-CPCR4-2 will be a valuable tracer for imaging the CXCR4 receptor status with PET.

DISCLOSURE STATEMENT

The costs of publication of this article were defrayed in part by the payment of page charges. Therefore, and solely to indicate this fact, this article is hereby marked "advertisement" in accordance with 18 USC section 1734.

ACKNOWLEDGMENTS

The expert advice of Prof. Dr. Sybille Ziegler and Dr. Behrooz H. Yousefi is gratefully acknowledged. We thank Katharina McGuire, Monika Beschorner, Andrea Alke, and Sybille Reder for their assistance. We also thank Dr. Amelie Lupp for their advice on and help with immunohistochemistry studies. Parts of this work were supported by the German Research Foundation (SFB 824/1-2009) and the Federal Ministry of Education and Research (MOBITECH/MOBITUM). No other potential conflict of interest relevant to this article was reported.

REFERENCES

1. Zlotnik A. Chemokines and cancer. *Int J Cancer.* 2006;119:2026–2029.
2. Burger JA, Kipps TJ. CXCR4: a key receptor in the crosstalk between tumor cells and their microenvironment. *Blood.* 2006;107:1761–1767.
3. Doitsidou M, Reichman-Fried M, Stebler J, et al. Guidance of primordial germ cell migration by the chemokine SDF-1. *Cell.* 2002;111:647–659.
4. Berger EA. Introduction: HIV co-receptors solve all questions and raise many new ones. *Semin Immunol.* 1998;10:165–168.
5. MacDermott RP. Chemokines in the inflammatory bowel diseases. *J Clin Immunol.* 1999;19:266–272.
6. Uchida D, Begum NM, Almofti A, et al. Possible role of stromal-cell-derived factor-1/CXCR4 signaling on lymph node metastasis of oral squamous cell carcinoma. *Exp Cell Res.* 2003;290:289–302.
7. Taichman RS, Cooper C, Keller ET, Pienta KJ, Taichman NS, McCauley RS. Use of the stromal cell-derived factor-1/CXCR4 pathway in prostate cancer metastasis to bone. *Cancer Res.* 2002;62:1832–1837.
8. Phillips RJ, Burdick MD, Lutz M, Belperio JA, Keane MP, Strieter RM. The stromal derived factor-1/CXCL12-CXC chemokine receptor 4 biological axis in non-small cell lung cancer metastases. *Am J Respir Crit Care Med.* 2003;167:1676–1686.
9. Zhan W, Liang Z, Zhu A, et al. Discovery of small molecule CXCR4 antagonists. *J Med Chem.* 2007;50:5655–5664.
10. Tamamura H, Xu Y, Hattori T, et al. A low-molecular-weight inhibitor against the chemokine receptor CXCR4: a strong anti-HIV peptide T140. *Biochem Biophys Res Commun.* 1998;253:877–882.

11. Zhu A, Zhan W, Liang Z, et al. Dipyrimidine amines: a novel class of chemokine receptor type 4 antagonists with high specificity. *J Med Chem.* 2010;53:8556–8568.
12. Tamamura H, Hiramatsu K, Ueda S, et al. Steroeselective synthesis of [L-Arg-L/D-3-(2-naphthyl)alanine]-type (E)-alkene dipeptide isosteres and its application to the synthesis and biological evaluation of pseudopeptide analogues of the CXCR4 antagonist FC131. *J Med Chem.* 2005;48:380–391.
13. Dijkgraaft I, Demmer O, Schumacher U, et al. CXCR4 receptor targeting for in-vivo imaging of metastases [abstract]. *J Nucl Med.* 2008;49(suppl):103P.
14. Wester HJ, Koglin N, Schwaiger M, Kessler H, Laufer B, Demmer O, Anton M, inventors; Technische Universität München, assignee. Cancer imaging and treatment. WO2007096662.
15. Wester HJ, Kessler H, Demmer O, Dijkgraaf I, inventors; Technische Universität München, assignee. Radiolabeled monomeric and multimeric cyclic oligopeptides binding to the CXCR4 receptor for cancer imaging and treatment. WO2009027706.
16. Hanaoka H, Mukai T, Tamamura H, et al. Development of a ^{111}In-labeled peptide derivative targeting a chemokine receptor, CXCR4, for imaging tumors. *Nucl Med Biol.* 2006;33:489–494.
17. Jacobson O, Weiss ID, Kiesewetter DO, Farber JM, Chen X. PET of tumor CXCR4 expression with 4-^{18}F-T140. *J Nucl Med.* 2010;51:1796–1804.
18. Jacobson O, Weiss ID, Szajek L, Farber J, Kiesewetter DO. ^{64}Cu-AMD3100: a novel imaging agent for targeting chemokine receptor CXCR4. *Bioorg Med Chem.* 2009;17:1486–1493.
19. Nimmagadda S, Pullamdhatla M, Stone K, Green G, Bhujwalla ZM, Pomper MG. Molecular imaging of CXCR4 receptor expression in human cancer xenografts with [^{64}Cu]AMD3100 positron emission tomography. *Cancer Res.* 2010;70:3935–3944.
20. Nimmagadda S, Pullambhatla M, Pomper MG. Immunoimaging of CXCR4 expression in brain tumor xenografts using SPECT/CT. *J Nucl Med.* 2009;50:1124–1130.
21. Misra P, Lebeche D, Ly H, et al. Quantitation of CXCR4 expression in myocardial infarction using ^{99m}Tc-labeled SDF-1α. *J Nucl Med.* 2008;49:963–969.
22. Demmer O, Gourni E, Schumacher U, et al. PET imaging of CXCR4 receptors in cancer by a new optimized ligand. *ChemMedChem.* 2011;6:1789–1791.
23. Demmer O, Dijkgraaf I, Schottelius M, Wester HJ, Kessler H. Introduction of functional groups into peptides via N-alkylation. *Org Lett.* 2008;10:2015–2018.
24. Schottelius M, Poethko T, Herz M, Kessler H, Schwaiger M, Wester HJ. First ^{18}F-labelled tracer suitable for routine clinical imaging of sst-receptor expressing tumors using positron emission tomography. *Clin Cancer Res.* 2004;10:3593–3606.
25. Wester HJ, Willoch F, Tölle TR, et al. 6-*O*-(2-[^{18}F]fluoroethyl)-6-*O*-desmethyldiprenorphine([^{18}F]DPN): synthesis, biological evaluation, and comparison with [^{11}C]DPN I humans. *J Nucl Med.* 2000;41:1279–1286.
26. Kalatskaya I, Berchiche YA, Gravel S, Limberg BJ, Rosenbaum JS, Heveker N. AMD3100 is a CXCR7 ligand with allosteric agonist properties. *Mol Pharmacol.* 2009;75:1240–1247.
27. Fischer T, Nagel F, Jacobs S, Stumm R, Schulz S. Reassessment of CXCR4 chemokine receptor expression in human normal and neoplastic tissues using the novel rabbit monoclonal antibody UMB-2. *PLoS ONE.* 2008;3:e4049.
28. Moepps B, Frodl R, Rodewald HR, Beggiolini M, Gierschik P. Two murine homologues of the human chemokine receptor CXCR4 mediating stromal cell-derived factor 1α activation of G_{i2} are differentially expressed in vivo. *Eur J Immunol.* 1997;27:2102–2112.
29. De León-Rodríguez LM, Kovacs Z. The synthesis and the chelation chemistry of DOTA-peptide conjugates. *Bioconjug Chem.* 2008;19:391–402.
30. Reubi JC, Schär J-C, Waser B, et al. Affinity profiles for human somatostatin receptor subtypes SST1-SST5 of somatostatin radiotracers selected for scintigraphic and radiotherapeutic use. *Eur J Nucl Med.* 2000;27:273–282.
31. Meyer GJ, Maecke HR, Schuhmacher J, Knaoo WH, Hofmann M. ^{68}Ga-labeled DOTA-derivatised peptide ligands. *Eur J Nucl Med Mol Imaging.* 2004;31:1097–1104.
32. Velikyan I, Andres S, Eriksson B, et al. In vivo binding of [^{68}Ga]-DOTATOC to somatostatin receptors in neuroendocrine tumors-impact of peptide mass. *Nucl Med Biol.* 2010;37:265–275.
33. Burns JM, Summers BC, Wang Y, et al. A novel chemokine receptor for SDF-1 and I-TAC involved in cell survival, cell adhesion, and tumor development. *J Exp Med.* 2006;203:2201–2213.
34. Thelen M, Thelen S. CXCR7, CXCR4 and CXCL12: an eccentric trio? *J Neuroimmunol.* 2008;198:9–13.
35. Nishizawa K, Nishiyama H, Oishi S, et al. Fluorescent imaging of high-grade bladder cancer using a specific antagonist for chemokine receptor CXCR4. *Int J Cancer.* 2010;127:1180–1187.
36. Weiss ID, Jacobson O, Kiesewetter DO, et al. Positron emission tomography imaging of tumors expressing the human chemokine receptor CXCR4 in mice. *Mol Imaging Biol*. February 23, 2011 [Epub ahead of print].
37. Froidevaux S, Eberle A, Christe M, et al. Neuroendocrine tumor targeting: study of novel gallium-labeled somatostatin radiopeptides in a rat pancreatic tumor model. *Int J Cancer.* 2002;98:930–937.
38. Akizawa H, Arano Y, Uezono T, et al. Renal metabolism of ^{111}In-DTPA-D-Phe1-octreotide in vivo. *Bioconjug Chem.* 1998;9:662–670.